PHILOSOPHICAL TRANSACTIONS OF THE ROYAL SOCIETY A MATHEMATICAL, PHYSICAL & ENGINEERING SCIENCES

Magnetic properties of strongly disordered electronic systems

Subir Sachdev

Phil. Trans. R. Soc. Lond. A 1998 **356**, 173-195
doi: 10.1098/rsta.1998.0156

The Royal Society

Magnetic properties of strongly disordered electronic systems

By Subir Sachdev

Department of Physics, Yale University, P.O. Box 208120, New Haven, CT 06520-8120, USA

We present a unified global perspective on the magnetic properties of strongly disordered electronic systems, with special emphasis on the case where the ground state is metallic. We review the arguments for the instability of the disordered Fermi liquid state towards the formation of local magnetic moments, and argue that their singular low temperature thermodynamics are the 'quantum Griffiths' precursors of the quantum phase transition to a metallic spin glass; the local moment formation is therefore not directly related to the metal–insulator transition. We also review the mean-field theory of the disordered Fermi liquid to metallic spin glass transition and describe the separate regime of 'non-Fermi liquid' behaviour at higher temperatures near the quantum critical point. The relationship to experimental results on doped semiconductors and heavy-fermion compounds is noted.

Keywords: quantum paramagnets; disordered metals; local moments; spin glasses

1. Introduction

This paper deals with the rich variety of magnetic phenomena and phases that appear in strongly disordered and correlated electronic systems in the vicinity of a metal–insulator transition. In particular, much attention has been focused on the ubiquitous 'local moments' which appear to dominate the low-temperature thermodynamics of the disordered metallic state, and also across the metal–insulator transition into the paramagnetic insulator (Quirt & Marko 1971; Ue & Maekawa 1971; Alloul & Dellouve 1987; Sachdev 1989; Milovanovic *et al.* 1989; Bhatt & Fisher 1992; Tusch & Logan 1993, 1995; Lakner *et al.* 1994; Langenfeld & Wolfle 1995). The principal thesis of this article is that these local moments are *not* directly related to the critical degrees of freedom leading to the metal–insulator transition. Rather, they should be understood as the 'quantum Griffiths' precursors of the transition from a disordered metal to a *metallic spin glass*.

Below, we will review the basic ideas needed to motivate and explain this thesis. We will also discuss a recent mean-field theory of the transition from the metal to the metallic spin glass (Sachdev *et al.* 1995; Sengupta & Georges 1995) and review its experimental consequences. We will not discuss the metal–insulator transition in the main part of the paper, but will speculate on the implications of our ideas for it in the concluding section.

2. General considerations at zero temperature

We will phrase our discussion in terms of the following Hamiltonian:

$$\mathcal{H} = -\sum_{i<j,\alpha} t_{ij} c^{\dagger}_{i\alpha} c_{i\alpha} + U \sum_{i} n_{i\uparrow} n_{i\downarrow} - \sum_{i,\alpha} (\epsilon_i - \mu) c^{\dagger}_{i\alpha} c_{i\alpha}, \tag{2.1}$$

Phil. Trans. R. Soc. Lond. A (1998) **356**, 173–195
Printed in Great Britain

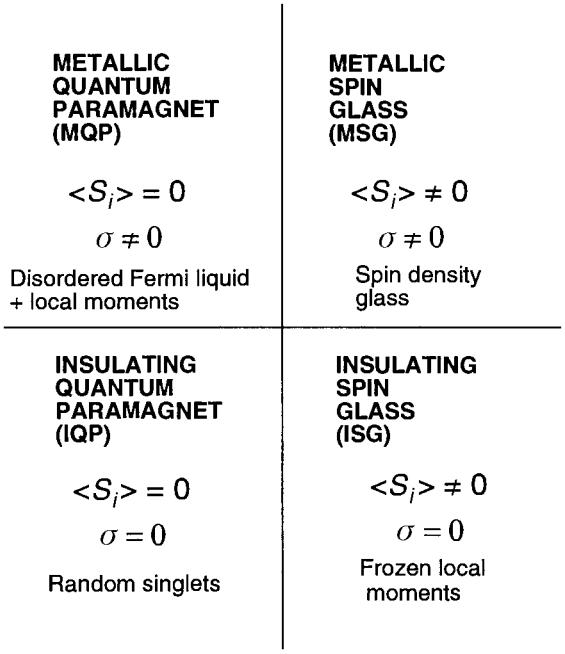

Figure 1. Schematic diagram of the $T = 0$ phases of a strongly random electronic system in three dimensions described, e.g. by the Hamiltonian (2.1). The average moment, $\langle S_i \rangle$, when non-zero, varies randomly from site to site. The conductivity is denoted by σ. The phase diagram is a section in the parameter space of $U/$(mean value of the t_{ij}), the width of the distribution of the t_{ij}, the range of the t_{ij} and the filling fraction.

where $c_{i\alpha}$ annihilates an electron on site i with spin $\alpha = \uparrow, \downarrow$, and $n_{i\alpha} = c^\dagger_{i\alpha} c_{i\alpha}$. The sites are placed in three-dimensional space and labelled by i, j. The electrons are in a chemical potential, μ, and repel each other with the on-site repulsion energy U. The hopping matrix elements between the sites are the t_{ij} which are short-ranged and possibly random. Finally, we also allow for some randomness in the on-site energies, ϵ_i. A Hamiltonian of the form of $\mathcal{H}$ is expected to be a good qualitative, if not quantitative, model of electronic motion in the impurity band of doped semiconductors, and this fact is the primary reason for focusing on it here. However, most of the discussion in this section is rather general and should apply to a wide variety of strongly disordered electronic systems.

We begin with a simple but important question: on general grounds, what are the different possible ground states of $\mathcal{H}$ between which it is possible to make a sharp distinction? Here we are considering two states distinct if a thermodynamic phase transition is required to connect one to the other. Notice also that we are referring to phases at *zero temperature* (T) so the phase transitions are necessarily quantum in nature. In some cases, two phases separated by a quantum phase transition at zero temperature can be connected smoothly at any non-zero temperature, and so the sharp distinctions made below are special to $T = 0$.

Figure 1 shows a schematic $T = 0$ phase diagram of $\mathcal{H}$ as its couplings are varied (an explicit computation of a related phase diagram on a cubic lattice has been presented by Tusch & Logan (1993, 1995)).

The phase diagram is a section in the parameter space of $U/\bar{t}$ (where $\bar{t}$ is the mean value of the t_{ij}), the width of the distribution of the t_{ij}, the range of the t_{ij} and the filling fraction. The phases are distinguished by the behaviour of their spin and

charge fluctuations. Charge transport is characterized by the $T = 0$ value of the conductivity, σ; if $\sigma = 0$ the phase is an insulator, and is metallic otherwise. For the spin sector, the uniform spin susceptibility is not a useful diagnostic (as will become clear below), and we distinguish phases by whether the ground state has infinite memory of the spin orientation on a site or not. The time-averaged moment on a given site is denoted by $\langle \boldsymbol{S}_i \rangle$, where

$$\boldsymbol{S}_i = c^{\dagger}_{i\alpha} \boldsymbol{\sigma}_{\alpha\beta} c_{j\beta}, \tag{2.2}$$

and $\boldsymbol{\sigma}$ are the Pauli matrices, and it can either vanish at every site or take a non-zero value which varies randomly from site to site. Experimentally, a phase with $\langle \boldsymbol{S}_i \rangle$ non-zero will have an elastic delta function at zero frequency in the neutron scattering cross section. The average over all sites will be denoted by $\overline{\langle \boldsymbol{S}_i \rangle}$, and will be non-zero only in ferromagnetic phases, which we will not consider here.

The four phases in figure 1 are as listed in the following four subsections.

(*a*) *Metallic quantum paramagnet (MQP)*

More simply known as the familiar 'metal', this phase has

$$\sigma \neq 0, \quad \langle \boldsymbol{S}_i \rangle = 0. \tag{2.3}$$

The standard picture of this phase is in terms of low energy excitations consisting of spin-$\frac{1}{2}$ charge-e fermionic itinerant quasi-particles. The quasi-particles obey a transport equation as in Landau's Fermi-liquid theory, but have wave functions which are spatially disordered. Many low-temperature transport properties of these quasi-particles have been computed in a weak disorder expansion (Altshuler & Aronov 1983; Finkelstein 1983, 1984; Castellani & DiCastro 1985; Belitz & Kirkpatrick 1994). Here, in § 3, we will review more recent work (Milovanovic *et al.* 1989; Bhatt & Fisher 1992; Lakner *et al.* 1994; Langenfeld & Wolfle 1995) that argues that this disordered Fermi liquid is in fact unstable towards the formation of 'local moments' of spin which modify most of its thermodynamic properties. A careful definition of a local moment, and its physical properties will appear in § 3, but loosely speaking, a local moment is a site with a strongly localized charge, e, and relatively slow spin fluctuations. The spin fluctuations, although long lived, eventually lose memory of their orientation, and we always have $\langle \boldsymbol{S}_i \rangle = 0$. There are large fluctuations in the lifetime of the spin orientations on the local moment sites, and those with the longest lifetimes may be considered as the 'quantum Griffiths' precursors (defined more carefully later) of the metallic spin glass to be considered below.

(*b*) *Insulating quantum paramagnet (IQP)*

This phase has

$$\sigma = 0, \quad \langle \boldsymbol{S}_i \rangle = 0, \tag{2.4}$$

and is accessed by a metal–insulator transition from the MQP phase. The itinerant quasi-particles have now localized: this prevents them from contributing to a DC conductivity, but many of their thermodynamic effects are expected to be similar to those in the MQP phase, particularly when the quasi-particle localization length is large. There is however no sharp distinction between the localized quasi-particles and the local moments, and at scales larger than the localization length one may view the IQP simply as a collection of randomly located spins with $S = \frac{1}{2}$ and interacting with one another by some effective exchange interaction. There is a large density of

low-energy spin excitations, which means that the spin susceptibility is quite large, and may even diverge as $T \to 0$ (Ma *et al.* 1979; Dasgupta & Ma 1980; Hirsch 1980; Bhatt & Lee 1982). This is the reason we have not used the spin susceptibility as a diagnostic for the phases. An exact solution of an IQP model with infinite-range exchange was presented recently by Sachdev & Ye (1993).

(*c*) *Metallic spin glass (MSG)*

This phase has

$$\sigma \neq 0, \quad \langle \boldsymbol{S}_i \rangle \neq 0, \tag{2.5}$$

and is accessed from the MQP by a spin-freezing transition. The local moments of the MQP phase now acquire a definite orientation and retain memory of this orientation for infinite time. The Fermi liquid quasi-particle excitations are still present and are responsible for the non-zero σ; the frozen moments appear as random local magnetic fields to the itinerant quasi-particles. Alternatively, we may view the spin-freezing transition as the onset, from the MQP phase, of a spin density wave with random offsets in its phase and orientation, as appears to be the case in recent experiments (Lamelas *et al.* 1995); this suggests the name '*spin density glass*'. The spin density glass point of view was explored by Hertz (1979) some time ago, but he did not focus on the vicinity of the $T = 0$ transition between the MSG and MQP phases. Here, in § 4 we will review the recent complete solution for the MSG phase and the MSG–MQP transition in the infinite range model (Sachdev *et al.* 1995; Sengupta & Georges 1995), aspects of the Landau theory for the short range case (Read *et al.* 1995; Sachdev *et al.* 1995), and recent experimental realizations. A more detailed review of this phase may be found elsewhere (Sachdev & Read 1996).

(*d*) *Insulating spin glass (ISG)*

This phase has

$$\sigma = 0, \quad \langle \boldsymbol{S}_i \rangle \neq 0. \tag{2.6}$$

Charge fluctuations are unimportant, and the collective frozen spin configuration is expected to be well described by an effective classical spin model. Examples of phases of this type may be found in well-known reviews (Binder & Young 1986; Fischer & Hertz 1991). We will not have anything to say about this phase here.

Let us emphasize that the above discussion was restricted to $T = 0$, and thus describes only the ground state properties of H. We will discuss the finite-T properties below. Well away from any of the quantum phase boundaries, the characteristics of the ground state are usually enough to give us a physical picture of the low-T properties. However, closer to the quantum phase boundaries or at higher T, entirely new regimes emerge which cannot be understood in terms of any of the phases describe above; rather, they are characterized by the critical states at the phase boundaries, and their universal response to temperature (Sachdev & Ye 1992; Sachdev 1995). This aspect of the physics will be explored in our discussion of the MQP–MSG quantum phase transition.

3. Formation of local moments in disordered metals

This section is about the magnetic properties of the MQP phase. The popular 'weakly disordered Fermi liquid' approach to this phase computes its low temperature properties by an expansion in the strength of the random elastic scattering by

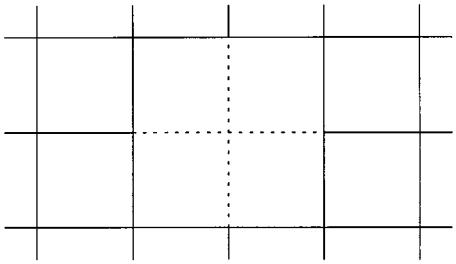

Figure 2. Hopping matrix elements of the single-impurity model considered in § 3 *a*. The dashed lines about the origin represent bonds with $t_{ij} = w$, while all remaining bonds have $t_{ij} = t$.

impurities (Altshuler & Aronov 1983; Finkelstein 1983, 1984; Castellani & DiCastro 1985; Belitz & Kirkpatrick 1994). The main purpose of this section is to show that this weak scattering expansion misses an important piece of physics that actually dominates the low-temperature thermodynamics and spin transport. The key phenomenon is the local instability of the interacting disordered Fermi liquid to the appearance of magnetic moments whose slow dynamics controls the long-time spin correlations. An essential property of this instability is that it is caused by fluctuations in the disorder strength over a small localized region of space; it is not related to any development of coherence over large spatial scales. It may be viewed as another realization of the general class of 'quantum Griffiths' effects which have been very important in numerous recent studies of quantum phases and phase transitions in random spin systems (Fisher 1992, 1995; Thill & Huse 1995; Read *et al.* 1995; Guo *et al.* 1996; Senthil & Sachdev 1996). In the present case these Griffiths effects are argued to be precursors of the metallic spin glass phase. That they disrupt what is usually considered to be an analysis of the metal–insulator transition is accidental: we argue they are not directly related to the metal–insulator transition and have clouded a proper interpretation of theories of it. We will begin by defining more carefully what we mean by a local moment in § 3 *a*. Then, in § 3 *b*, we will describe the current theoretical understanding of the formation of these local moments in random systems, and their implications for experiments.

(*a*) *What is a local moment?*

Unlike the sharply distinguishable zero temperature phases that were discussed in § 2, the concept of a local moment initially appears somewhat imprecise, and refers to intermediate energy phenomena at moderate non-zero temperatures. Alternatively, we may take a renormalization group point of view, and introduce local moments, as one renormalizes down from higher energies, as the degrees of freedom necessary for a proper description of the low energy excitations about the ground state. Despite this seeming imprecision, as we shall see below, the presence of local moments does lead to a qualitatively different description of the low temperature properties of disordered metals.

To explain the concept further, it is useful to specialize to a particular realization of $\mathcal{H}$ (Milovanovic *et al.* 1989): a single impurity model related to models considered early on by Anderson (1961) and Wolff (1961). Place all the sites, i, on the vertices of a regular lattice, and set $\epsilon_i = 0$, $t_{ij} = t$ between all nearest neighbours, and $t_{ij} = 0$ otherwise. Now pick a special 'impurity' site $i = 0$, and set all its nearest neighbour bonds $t_{0i} = w$ (see figure 2).

We choose the chemical potential $\mu = -\frac{1}{2}U$ so that the system is half filled, and

the resulting model is now characterized by two dimensionless parameters: w/t and U/t. We will now argue, using the results of extensive numerical and analytic studies on closely related models (Haldane 1978; Krishnamurthy *et al.* 1980), that there are two qualitatively distinct regimes in the w/t and U/t plane, characterized by very different behaviour in their non-zero temperature properties.

We will characterize the two regions by their local spin susceptibility, $\chi_{\rm L}$. This is their response to a magnetic field coupled to site 0 under which

$$\mathcal{H} \to \mathcal{H} - \tfrac{1}{2} g\mu_{\rm B} H (c^\dagger_{0\uparrow} c_{0\uparrow} - c^\dagger_{0\downarrow} c_{0\downarrow}). \tag{3.1}$$

First consider the very-high-temperature limit $T \gg t, U, w$. In this case all states are equally probably. On site 0 there are four possible configurations: empty, two electrons, one spin-up electron, and one spin-down electron. Of these, the latter two contribute a standard Curie susceptibility of $(g\mu_{\rm B})^2/(4k_{\rm B}T)$, while the first two have zero susceptibility. The average high temperature susceptibility is therefore

$$\chi_{\rm L} = \frac{(g\mu_{\rm B})^2}{8k_{\rm B}T}, \quad T \gg U, t, w. \tag{3.2}$$

Now lower the temperature. The implication of the earlier work (Anderson 1961; Wolff 1961; Haldane 1978; Krishnamurthy *et al.* 1980) is that there are two distinct possibilities in the w/t, U/t phase diagram as described in the following two subsubsections.

(i) *Itinerant quasi-particle regime*

The value of $T\chi_{\rm L}$ decreases monotonically from the high-T limit (3.2) as T is lowered. The states at site 0 are absorbed into the itinerant quasi-particle states of the surrounding sites, and the excitations at 0 are typical of those of a Fermi liquid. As $T \to 0$ we therefore expect the constant Pauli susceptibility $\chi_{\rm L} \sim (g\mu_{\rm B})^2/E_{\rm F}$ where $E_{\rm F} \sim t$ is the Fermi energy. Therefore $T\chi_{\rm L} \to 0$ as $T \to 0$. This regime is clearly connected to the $w = t$ point where site 0 ceases to be special.

(ii) *Local moment regime*

Now as T is lowered below $T \sim U$, the value of $T\chi_{\rm L}$ rises and reaches a plateau where

$$T\chi_{\rm L} = \frac{(g\mu_{\rm B})^2}{4k_{\rm B}T}, \quad T_{\rm K} \ll T \ll U. \tag{3.3}$$

(The lower limit is the Kondo temperature, $T_{\rm K}$, and will be discussed below.) The natural interpretation of this plateau is that two of the four possible states at site 0 have been suppressed: site 0 either has one spin-up electron or one spin-down electron, and it is extremely unlikely that it is in the state with no electrons or with two electrons in a spin-singlet state. When this happens, we assert that a local moment has formed at site 0. Note that this strong local correlation between the spin-up and spin-down occupations is not compatible with an itinerant fermionic quasi-particle description, and really requires one to think in terms of a fluctuating spin (a local moment) at site 0. As the temperature is lowered further in this regime, the non-trivial physics of the Kondo effect becomes active at temperatures of order $T_{\rm K} \sim t\exp(-cUt/w^2)$ where c is a constant of order unity. Notice that this temperature is exponentially small for large U, and the temperature range in (3.3) is well defined. At temperatures below $T_{\rm K}$ the local moment at 0 is quenched by the formation of a

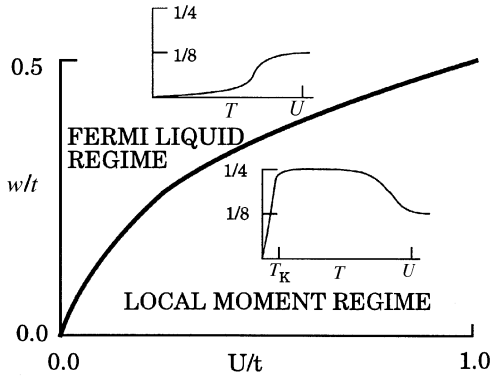

Figure 3. Mean field phase diagram of the single impurity Hubbard model sketched in figure 2. The solid line represents a smooth crossover which appears as a sharp transition in the mean-field theory. The insets plot the values of $T\chi_{\mathrm{L}}$ in the two regimes. (From Milovanovic *et al.* 1989.)

spin singlet with an electron drawn from the conduction band. The local suscepbility therefore eventually returns to that of the Pauli susceptibility of a Fermi liquid.

Notice that as $T \to 0$, there is no sharp distinction between cases (i) and (ii) above: in both cases the spin susceptibility is that of a Fermi liquid. Nevertheless, there is a significant difference in the intermediate temperature behaviour. In the original mean-field theory of Anderson (1961) this distinction between the two cases appears as a sharp phase transition, but this is an artifact of the mean-field approximation. We show in figure 3 the phase diagram of the single impurity model as determined by the generalization of the Anderson (1961) mean-field theory.

Also sketched are the behaviours of $T\chi_{\mathrm{L}}$ outlined above.

It is also useful to notice the analogy between the features noted above and the fluctuations which lead to the quantum Griffiths singularities in random spin systems (Fisher 1992, 1995; Thill & Huse 1995; Read *et al.* 1995; Guo *et al.* 1996; Senthil & Sachdev 1996). In the latter cases the important random fluctuations are in localized regions in which the quantum spin correlations have their values enhanced by some finite fraction. As above, the contribution of any single such region is eventually quenched by its quantum coupling to the surrounding spins. The true importance of the local random fluctuations, and the qualitative difference they make to the macroscopic properties, only becomes apparent when the collective statistics of the global system is examined. We will turn to this in the following subsection.

(*b*) *Instabilities in the fully disordered model*

Now we turn to the full complexity of $\mathcal{H}$, allowing the configuration of every site to be random. We anticipate that quantum Griffiths effects noted above could have an important influence here, but before we can apply such arguments, more elementary issues need to be settled.

(i) Do the single impurity instabilities discussed above apply to the fully random case, in which every site is potentially an impurity site?

(ii) What is the spatial extent of each local moment instability? In particular, is it correlated with the localization length of the itinerant quasi-particles?

(iii) Is it valid to treat the different instabilities independently of each other?

Although the possibile importance of local moments to disordered metals had been noted earlier (Quirt & Marko 1971; Ue & Maekawa 1971; Alloul & Dellouve 1987;

Sachdev 1989), these questions were first addressed by Milovanovic *et al.* (1989), and we review their results below.

First, notice that the distinction between the two regimes of the single-impurity model became apparent at a relatively high temperature $T \sim U$. The same feature is expected to hold in the fully disordered model, and we will therefore treat the interactions in $\mathcal{H}$ within the Hartree–Fock approximation. It is essential, however, to include the effects of disorder exactly: this approach is therefore the converse of the method used to describe the disordered itinerant quasi-particles (Altshuler & Aronov 1983; Finkelstein 1983, 1984; Castellani & DiCastro 1985; Belitz & Kirkpatrick 1994). A useful way to formulate the Hartree–Fock or 'self-consistent field' approach is to consider it as the optimization of a single-particle effective Hamiltonian $\mathcal{H}_{\rm eff}$. We choose this in the form

$$\mathcal{H} = -\sum_{i<j,\alpha} t_{ij} c^{\dagger}_{i\alpha} c_{i\alpha} + \sum_{i} (\tilde{\epsilon}_i - \mu) c^{\dagger}_{i\alpha} c_{i\alpha} - \sum_{i} \boldsymbol{h}_i \cdot \boldsymbol{S}_i, \tag{3.4}$$

where $\tilde{\epsilon}_i$ and $\boldsymbol{h}_i$ are the variational parameters. Notice that the $\boldsymbol{h}_i$ are local magnetic fields which polarize the electrons on site i. The appearance of a significant $\boldsymbol{h}_i$ on a given site is the signal of a formation of a local moment, and the spatial form of the $\boldsymbol{h}_i$ field therefore contains the essential information that we want. As we are mainly discussing the issue of the initial instability towards the formation of local moments, it is useful to expand the effective free energy in powers of the $\boldsymbol{h}_i$. The results of such an expansion are

$$\mathcal{F}_{\rm eff}(\boldsymbol{h}_i) = \mathcal{F}_0 + \frac{1}{4} \sum_{i,j,k} \chi_{ij} (\delta_{jk} - U \chi_{jk}) \boldsymbol{h}_i \cdot \boldsymbol{h}_k + \mathcal{O}(\boldsymbol{h}^4), \tag{3.5}$$

where $\mathcal{F}_0$ is the free energy of the unpolarized state with $\boldsymbol{h}_i = 0$. The quantity χ_{ij} is the spin susceptibility matrix of this unpolarized state—it is the response in the magnetization at site i to a magnetic field at site j. More specifically, it is defined by

$$\chi_{ij} = \sum_{\alpha,\beta} \Psi_\alpha(i)\, \Psi^*_\beta(i)\, \Psi^*_\alpha(j)\, \Psi_\beta(j) \frac{f(\lambda_\alpha) - f(\lambda_\beta)}{\lambda_\beta - \lambda_\alpha}, \tag{3.6}$$

where $f(\lambda)$ is the Fermi function, $\Psi_\alpha(i)$ are the wavefunctions of the itinerant quasi-particles in the unpolarized state, and λ_α are their energies. In the present effective field approximation these are the eigenvalues and eigenenergies of a one-particle Hamiltonian

$$\sum_j [(\tilde{\epsilon}_i - \mu)\delta_{ij} - t_{ij}]\, \Psi_\alpha(j) = \lambda_\alpha\, \Psi_\alpha(i). \tag{3.7}$$

Finally, the parameters $\tilde{\epsilon}_i$ are determined by the nonlinear self-consistency condition

$$\tilde{\epsilon}_i = \epsilon_i + U \sum_\alpha |\, \Psi_\alpha(i)|^2 f(\lambda_\alpha). \tag{3.8}$$

The equations (3.7) and (3.8) were solved numerically for realistic realizations of the disorder appropriate to Si:P. The density of the disorder was chosen so that the system is comfortably within the metallic phase. The quasi-particle wavefunctions, Ψ_α, are extended for a wide range of energies near the Fermi level, and explicit evidence is presented for this below. From the known Ψ_α and λ_α, the susceptibility matrix χ_{ij} was determined from (3.6).

To proceed further, is is useful to now diagonalize χ_{ij}. We solve the eigenvalue problem

$$\chi_{ij} m_a(j) = \kappa_a m_a(j), \tag{3.9}$$

where κ_a are the eigenvalues, and m_a are the normalized eigenvectors. Now make the expansion

$$\boldsymbol{h}_i = \sum_a \boldsymbol{p}_a m_a(i) \tag{3.10}$$

and insert it into (3.5). We get

$$\mathcal{F} = \mathcal{F}_0 + \frac{1}{4} \sum_a \kappa_a (1 - U\kappa_a) \boldsymbol{p}_a^2 + \mathcal{O}(\boldsymbol{p}^4). \tag{3.11}$$

We see that there is first an instability to a non-zero value of $\boldsymbol{p}_a$ if the associated eigenvalue $\kappa_a > 1/U$. We identify the temperature at which this first happens with the formation of a local moment with spatial distribution of spin proportional to $m_a(i)$. What now happens at lower temperatures depends upon the spatial structure of $m_a(i)$. If all of the instabilities appear in *localized* eigenvectors $m_a(i)$ which are spatially well separated from each other, then they are approximately decoupled, and we can identify the formation of each of those local moments at the point where their respective $\kappa_a > 1/U$. On the other hand, if any of the $m_a(i)$ are extended, then we have to go into the magnetized phase with $\boldsymbol{p}_a = 0$, recompute the new susceptibility matrix, and diagonalize it again. The latter possibility in fact corresponds to the appearance of the long-range order of the metallic spin glass phase, and will be discussed in § 4. In the present circumstances we found that all the m_a were indeed well localized.

Evidence for the localization is presented in figure 4. There we compare the values of the inverse participation ratios $P_{\mathcal{H}}$ and P_χ which are defined by

$$P_{\mathcal{H}} = \left\langle \sum_i |\Psi_\alpha(i)|^4 \right\rangle, \quad P_\chi = \left\langle \sum_i |m_a(i)|^4 \right\rangle. \tag{3.12}$$

The eigenstates $\Psi_\alpha(i)$ and $m_a(i)$ are both normalized, and so $P_{\mathcal{H},\chi}$ are measures of their average spatial extent. If the states are localized then $P_{\mathcal{H},\chi}$ will saturate to some finite value of order unity as the system size is increased; on the other hand, if the states are extended, we expect $P_{\mathcal{H},\chi}$ to roughly decrease as $1/N$ where N is the number of sites. We see from figure 4 that the behaviour of the two participation ratios is dramatically different. The quasi-particle wavefunctions $\Psi_\alpha(i)$ are clearly extended, as has been previously claimed. For the same samples, however, the $m_a(i)$ are well localized, on the scale of just one or two sites ($P_\chi \sim 0.5$).

The localization of the $m_a(i)$ is the key result of the numerical analysis of Milovanovic *et al.* (1989). It answers the questions posed at the beginning of this subsection. This localization justifies the identification of the instabilities in the fully random $\mathcal{H}$ and $\mathcal{H}_{\text{eff}}$ with essentially independent instabilities, much like those in the single-impurity model. The local moments are confined to just a few sites, and this localization is quite independent of the localization length of the quasi-particles, which are in fact itinerant. The initial instabilities at different points in the sample are essentially decoupled as they correspond to different localized eigenvectors of χ_{ij} with little mutual overlap. All of these features are again consistent with their interpretation as Griffiths effects which require rare *independent* fluctuations in different regions of the sample. All Griffiths effects are precursors of some actual phase

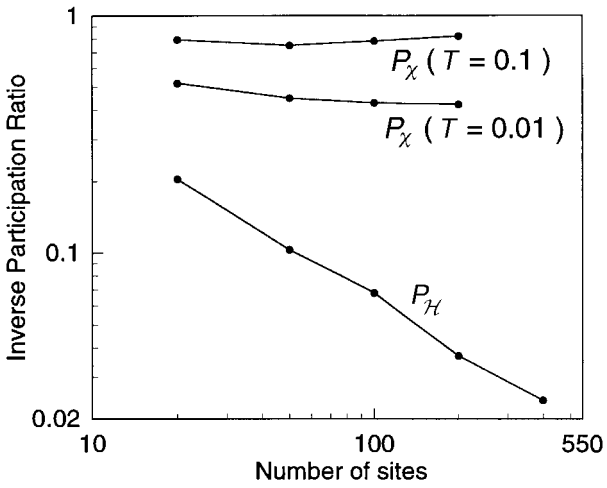

Figure 4. Evidence for the localization of the magnetization eigenvectors in the metallic phase. The inverse participation ratios of the eigenvectors of the susceptibility (P_χ) and the quasi-particle Hamiltonian ($P_{\mathcal{H}}$) plotted as a function of system size. Notice that the magnetic modes are well localized as P_χ is roughly independent of system size, while the quasi-particle excitations are extended as $P_{\mathcal{H}}$ decreases rapidly with system size (from Milovanovic *et al.* 1989).

transition, the proper identification of which requires some understanding of lower temperature properties of the local moments, which we address in the next section.

(*c*) *Low-temperature thermodynamics of local moments*

Once the local moments have formed at temperatures $T \sim U$, a different effective Hamiltonian for the low temperature properties of the metal is clearly warranted. On the local moment sites, states with two spin singlet electrons, or with no electrons, occur only with a small probability, and it will clearly pay to eliminate them by a canonical transformation. Let us denote that sites upon which we want to perform this canonical transformation by ℓ. Then on each such site, ℓ, we have only two allowed states: a spin-up electron or a spin-down electron, and a quantum spin-$\frac{1}{2}$ operator $\boldsymbol{S}_\ell$ which transforms among them.

We have assumed above that the local moment resides on a single site. It is clearly possible to have moments located on two or more sites but we expect that a similar procedure can be applied. A higher spin-j operator might be required, and more states may have to be eliminated, but these complications are not expected to modify any of the following discussion.

We can now write down an effective Hamiltonian for the entire random system

$$\mathcal{H}_{\mathrm{K}} = -\sum_{i<j,\alpha}{}' t_{ij} c^\dagger_{i\alpha} c_{i\alpha} + U \sum_i{}' n_{i\uparrow} n_{i\downarrow} - \sum_{i,\alpha}{}' (\epsilon_i - \mu) c^\dagger_{i\alpha} c_{i\alpha} + \sum_i{}' \sum_\ell J_{i\ell} \boldsymbol{S}_\ell \cdot c^\dagger_{i\alpha} \boldsymbol{\sigma}_{\alpha\beta} c_{i\beta}. \tag{3.13}$$

The primes on the sums indicate that the sites ℓ have to be excluded from the sum over i. The new feature is the Kondo exchange coupling, $J_{i\ell}$ (expected to be antiferromagnetic) between the local moments and the itinerant electrons, and this is the remnant of the canonical transformation eliminating the states on the local moment sites. The low-temperature properties of random models like $\mathcal{H}_{\mathrm{K}}$ have been considered by a number of investigators (Bhatt & Fisher 1992; Dobrosavljevic *et al.*

1992; Dobrosavljevic & Kotliar 1993; Tusch & Logan 1993, 1995; Lakner *et al.* 1994; Langenfeld & Wolfle 1995; Rowan *et al.* 1995; Miranda *et al.* 1996, 1997)

We will focus here on the elegant results of Lakner *et al.* (1994) and Langenfeld & Wolfle (1995) which have the virtue of containing *quantitative* predictions specific to Si:P. They began with a quantitative computation of the boundary between the single impurity local moment and itinerant quasi-particle regimes in environments characteristic of those found in Si:P. Assuming that the location of the P sites in Si:P were statistically uncorrelated, they computed the probability distributions of the local environments of the sites. The combination of these results allowed to predict two quantities essential for a quantitative comparison with experimental results: (i) the density of local moments as a function of P doping; and (ii) the probability distribution of the Kondo temperatures $\mathcal{P}(T_{\rm K})$ of these local moment sites. Over a broad range of $T_{\rm K}$ values, including the entire experimentally relevant range, they found that

$$\mathcal{P}(T_{\rm K}) = \frac{c_0}{T_K^{\alpha_{\rm K}}}, \tag{3.14}$$

where c_0 is a normalization constant and $\alpha_{\rm K} \approx 0.9$. If one now ignores the possible exchange couplings between the local moments (these could be mediated by the itinerant quasi-particles, or due to a direct exchange), the local moment contribution to thermodynamic properties can be computed by a simple superposition of the universal single impurity thermodynamics at different Kondo temperatures. Such a procedure gives a specific heat $C \sim T^{1-\alpha_{\rm K}}$ and a uniform spin susceptibility $\chi \sim T^{-\alpha_{\rm K}}$. Lakner *et al.* (1994) find good quantitative agreement between such model calculations and experimental measurements of the specific heat.

The singular low-temperature effects of the local moments above are clearly associated with those sites at which $T_{\rm K}$ is anomalously small. The local spin orientation on those sites has a long lifetime, and under these conditions any RKKY coupling between them will clearly be important, although it has been neglected in the above analyses. Indeed this RKKY coupling will prefer a fixed relative orientation among the slowly fluctuating moments. As the RKKY coupling is an oscillating function of separation, the relative orientation will oscillate in sign. Taking the limit over which this RKKY coupling correlates an increasingly larger number of local moments, we see that eventually spin glass order will appear. None of this incipient ordering has directly involved the itinerant quasi-particles, and so the system will remain metallic. These arguments clearly show that the Griffiths effects associated with local moment formation are precursors of the metallic spin glass phase.

4. Metallic spin glasses

We now turn to an analysis of the metallic spin glass (MSG), with a particular focus on its transition to the metallic phase (MQP) and the crossovers at finite temperature in the vicinity of the quantum critical point. This analysis will be done within the framework of a Landau theory for this transition that was developed recently (Read *et al.* 1995; Sachdev *et al.* 1995). Such analysis effectively focuses only on the extended eigenmodes of the susceptibility χ_{ij} into which there is condensation in the spin glass phase. The quantum Griffiths effects that were crucial to understanding the low-temperature properties of the MQP are entirely missing at the mean-field level. Omission of these Griffiths effects is probably quite dangerous at low temperatures. However, we shall find new regimes at moderate temperatures which display novel

physics associated with the extended states of the critical point, and the analysis below should be considered a first attempt towards their understanding.

Portions of the discussion below are adapted from the recent review article by Sachdev & Read (1996) and the reader is referred to it for greater detail. We shall take a Landau theory point of view in this article and hence automatically obtain a formalism which is suited for analysis of fluctuations (Sachdev *et al.* 1995; Sachdev & Read 1996). However it is also possible to obtain results equivalent to those of the Landau mean-field theory by the exact solution of an infinite-range model: such an approach was followed by Sengupta & Georges (1995) (and also for related models by Huse & Miller (1993) and Ye *et al.* (1993)), but we shall not use it here.

In the following subsections we will: (i) introduce the order parameter for quantum spin glass to paramagnet transition; (ii) obtain a Landau functional for this order parameter; (iii) minimize the functional as a function of temperature and coupling constant to obtain the predictions of crossover functions; and (iv) briefly discuss the relationship to recent experiments on heavy fermion compounds.

(*a*) *Order parameter*

We begin by introducing the order parameter for the quantum phase transition (Read *et al.* 1995). Recall that for classical spin glasses in the replica formalism, this is a matrix q^{ab}, $a, b = 1 \ldots n$ are replica indices and $n \to 0$. The *off-diagonal* components of q^{ab} can be related to the Edwards–Anderson order parameter, $q_{\rm EA}$, in a somewhat subtle way that we will not go into here (Fischer & Hertz 1991; Binder & Young 1986). In quantum ($T = 0$) phase transitions, time-dependent fluctuations of the order parameter must be considered (in 'imaginary' Matsubara time τ), and in the spin glass case it is found that the standard decoupling, analogous to the classical case introducing q^{ab}, leads now to a matrix function of two times (Bray & Moore 1980) which we can consider to be

$$Q^{ab}(x, \tau_1, \tau_2) = \sum_{i \in \mathcal{N}(x)} S_i^a(\tau_1) S_i^b(\tau_2), \tag{4.1}$$

where $\mathcal{N}(x)$ is a coarse-graining region in the neighborhood of x, and we will henceforth omit the vector spin indices on all operators except where necessary. From the set-up of the replica formalism it is clear that

$$\overline{\langle S_i(0) \cdot S_i(\tau) \rangle} = \lim_{n \to 0} \frac{1}{n} \sum_a \langle\langle Q^{aa}(x, \tau_1 = 0, \tau_2 = \tau) \rangle\rangle, \tag{4.2}$$

$$q_{\rm EA} = \lim_{\tau \to \infty} \lim_{n \to 0} \frac{1}{n} \sum_a \langle\langle Q^{aa}(x, \tau_1 = 0, \tau_2 = \tau) \rangle\rangle, \tag{4.3}$$

relating $q_{\rm EA}$ to the replica *diagonal* components of Q. We have introduced above double angular brackets to represent averages taken with the translationally invariant replica action (recall that single angular brackets represent thermal/quantum averages for a fixed realization of randomness and overlines represent averages over randomness). Notice that the fluctuating field Q is in general a function of two separate times τ_1 and τ_2; however the expectation value of its replica diagonal components can only be a function of the time difference $\tau_1 - \tau_2$. Further, the expectation value of the replica off-diagonal components of Q is independent of both τ_1 and τ_2 (Ye *et al.* 1993), and has a structure very similar to that of the classical order parameter q^{ab}. One can therefore also obtain $q_{\rm EA}$ from the replica off-diagonal components of

Q, as noted above for q^{ab}. Let us also note for completeness that, unlike the quantum case, the replica diagonal components of the classical order parameter q^{ab} are usually constrained to be unity and contain no useful information.

The order parameter we shall use is $Q^{ab}(x, \tau_1, \tau_2)$, which is a matrix in a replica space and depends on the spatial coordinate x and two times τ_1, τ_2. However, a little thought shows that this function contains too much information. The important degrees of freedom, for which one can hope to make general and universal statements, are the long-time spin correlations with $|\tau_1 - \tau_2| \gg \tau_{\mathrm{m}}$, where τ_{m} is a microscopic time like an inverse of a typical exchange constant. As presented, the function Q contains information not only on the interesting long-time correlations, but also on the uninteresting time range with $|\tau_1 - \tau_2|$ smaller than or of order τ_{m}. The correlations in the latter range are surely model dependent and cannot be part of any general Landau action. We shall separate out this uninteresting part of Q by performing the shift

$$Q^{ab}(x, \tau_1, \tau_2) \rightarrow Q^{ab}(x, \tau_1, \tau_2) - C\delta^{ab}\delta(\tau_1 - \tau_2), \tag{4.4}$$

where C is a constant, and the delta function $\delta(\tau_1 - \tau_2)$ is a schematic for a function which decays rapidly to zero on a scale τ_{m}. The value of C will be adjusted so that the resulting Q contains only the interesting long-time physics: we will see later how this can be done in a relatively straightforward manner. The alert reader may recognize some similarity between the above procedure, and the analysis of Fisher (1978) of the Yang–Lee edge problem. In that case, too, the order parameter contains an uninteresting non-critical piece which has to be shifted away; we will see below that there are many other similarities between the Yang–Lee edge and quantum spin glass problems.

(*b*) *Action functional*

The action functional can be derived by explicit computations on microscopic models or deduced directly from general arguments which have been discussed in some detail by Read *et al.* (1995). Apart from a single non-local term present in the metallic case (Sachdev *et al.* 1995, see below), the remaining important terms are consistent with the general criteria as follows.

(i) The action is an integral over space of a local operator which can be expanded in gradients of powers of Q evaluated at the same position x;

(ii) Q is bilocal (i.e. is a matrix) in time, and each time is associated with one of the two replica indices (see definition equation (4.1)). These 'indices' can appear more than once in a term and are summed over freely subject to the following rules before summations:

(a) each distinct replica index appears an even number of times;

(b) repetition of a time 'index' corresponds to quantum-mechanical interaction of spins, which must be local in time and accordingly can be expanded as terms with times set equal plus the same with additional derivatives—it occurs when the corresponding replica indices are the same, and only then.

We now present all the terms, which, a subsequent renormalization-group analysis tells us are important near the quantum critical point. This is only a small subset of the terms allowed by the above criteria.

A crucial term is the linear one in the order parameter Q. This term encodes the local on-site physics of the spin glass model, and tells us that the spin is coupled to

a metallic bath of itinerant quasi-particles.

$$\frac{1}{\kappa t}\int \mathrm{d}^d x\left\{\int \mathrm{d}\tau \sum_a \tilde{r} Q^{aa}(x,\tau,\tau) - \frac{1}{\pi}\int \mathrm{d}\tau_1 \mathrm{d}\tau_2 \sum_a \frac{Q^{aa}(x,\tau_1,\tau_2)}{(\tau_1-\tau_2)^2}\right\}. \tag{4.5}$$

The coupling $\tilde{r}$ will be seen below to be the critical tuning parameter for the transition from the spin glass to the paramagnet. There is an overall factor of $1/\kappa t$ in front of this term; we have written this factor as a product of two coupling constants, κ and t, for technical reasons we shall not discuss here.

There is a quadratic gradient term

$$\frac{1}{2t}\int \mathrm{d}^d x \mathrm{d}\tau_1 \mathrm{d}\tau_2 \sum_{a,b} [\nabla Q^{ab}(x,\tau_1,\tau_2)]^2, \tag{4.6}$$

which is responsible for the development of spatial correlations in the spin glass order. A quadratic term without gradients,

$$\int \mathrm{d}^d x \mathrm{d}\tau_1 \mathrm{d}\tau_2 \sum_{a,b} [Q^{ab}_{\mu\nu}(x,\tau_1,\tau_2)]^2, \tag{4.7}$$

is also allowed by the general criteria, but we choose to tune its coefficient to zero by using the freedom in (4.4). As will become clear in the next subsection, this criterion is identical to requiring the absence of uninteresting short-time behaviour in Q. Notice again the formal similarity to the theory of the Yang–Lee edge (Fisher 1978), where setting the coefficient of a quadratic term to zero was also responsible for removing the uninteresting non-critical part of the order parameter variable.

Next we consider cubic non-linearities, and the most important among the several allowed terms is the one with the maximum number of different time and replica indices:

$$-\frac{\kappa}{3t}\int \mathrm{d}^d x \mathrm{d}\tau_1 \mathrm{d}\tau_2 \mathrm{d}\tau_3 \sum_{a,b,c} Q^{ab}(x,\tau_1,\tau_2) Q^{bc}(x,\tau_2,\tau_3) Q^{ca}(x,\tau_3,\tau_1). \tag{4.8}$$

This term accounts for nonlinearities induced solely by disorder fluctuations.

Of the terms with fewer than the maximum allowed number of time indices at a given order, the most important one is the one at quadratic order:

$$\frac{u}{2t}\int \mathrm{d}^d x \mathrm{d}\tau \sum_a u Q^{aa}(x,\tau,\tau) Q^{aa}(x,\tau,\tau). \tag{4.9}$$

The coupling u is the only one responsible for quantum mechanical interactions between the spins, and as a consequence, all the time and replica indices in (4.9) are the same.

Lastly we have a final quadratic term

$$-\frac{1}{2t^2}\int \mathrm{d}^d x \int \mathrm{d}\tau_1 \mathrm{d}\tau_2 \sum_{a,b} Q^{aa}(x,\tau_1,\tau_1) Q^{bb}(x,\tau_2,\tau_2), \tag{4.10}$$

which accounts for the spatial fluctuation in the position of the paramagnet spin glass transition. Recall that the linear coupling $\tilde{r}$ was the control parameter for this transition, and a term like (4.10) is obtained by allowing for Gaussian fluctuations in $\tilde{r}$, about its mean value, from point to point in space. It will turn out that (4.10) plays no role in the mean-field analysis in the following subsection. However, it is essential to include (4.10) for a proper theory of the fluctuations.

The final Landau theory of the metallic spin glass and its transition to the metal is then (4.5)–(4.10).

(*c*) *Mean field theory*

We will now minimize the action of § 4 *b*. We will review the mean-field theory for the MQP phase and identify the position of its instability to the MSG phase. A discussion of the solution within the MSG phase will not be presented here.

We Fourier transform from imaginary time to Matsubara frequencies by expressing the action in terms of

$$Q^{ab}(x,\omega_1,\omega_2)=\int_0^{1/T}\mathrm{d}\tau_1\mathrm{d}\tau_2 Q^{ab}(x,\tau_1,\tau_2)\mathrm{e}^{-\mathrm{i}(\omega_1\tau_1+\omega_2\tau_2)}, \tag{4.11}$$

where we are using units in which $\hbar = k_{\mathrm{B}} = 1$, and the frequencies, ω_1, ω_2 are quantized in integer multiples of $2\pi T$. Then, we make an ansatz for the mean-field value of Q which is x independent, and dependent only on $\tau_1 - \tau_2$; within the MQP phase this takes the form

$$Q^{ab}(x,\omega_1,\omega_2)=(\delta^{ab}\delta_{\omega_1+\omega_2,0}/T)\chi_{\mathrm{L}}(\mathrm{i}\omega_1), \tag{4.12}$$

where we have used (4.3) to identify the right-hand side as the local dynamic susceptibility. Inserting (4.12) into the action for the metallic case in § 4 *b*, we get for the free energy per unit volume $\mathcal{F}/n$ (as usual, $\mathcal{F}/n$ represents the physical disorder averaged free energy):

$$\frac{\mathcal{F}}{n}=\frac{T}{t}\sum_{\omega}\left[\frac{|\omega|+\tilde{r}}{\kappa}\chi_{\mathrm{L}}(\mathrm{i}\omega)-\tfrac{1}{3}\kappa\chi_{\mathrm{L}}^3(\mathrm{i}\omega)\right]+\frac{u}{2t}\left[T\sum_{\omega}\chi_{\mathrm{L}}(\mathrm{i}\omega)\right]^2. \tag{4.13}$$

Notice that the coupling $1/t$ appears only as a prefactor in front of the total free energy, as the contribution of the $1/t^2$ term (4.10) vanishes in the replica limit $n \to 0$. The value of t will therefore play no role in the mean-field theory. We now determine the saddle point of (4.13) with respect to variations in the whole function $\chi_{\mathrm{L}}(\mathrm{i}\omega)$, and find the solution

$$\chi_{\mathrm{L}}(\mathrm{i}\omega)=-\frac{1}{\kappa}\sqrt{|\omega|+\Delta}, \tag{4.14}$$

where the energy scale Δ is determined by the solution of the equation

$$\Delta=\tilde{r}-uT\sum_{\omega}\sqrt{|\omega|+\Delta}. \tag{4.15}$$

Taking the imaginary part of the analytic continuation of (4.14) to real frequencies, we get

$$\chi_{\mathrm{L}}''(\omega)=\frac{1}{\kappa\sqrt{2}}\frac{\omega}{\sqrt{\Delta+\sqrt{\omega^2+\Delta^2}}}. \tag{4.16}$$

Inserting the solution for χ_{L} back into (4.13), and using (4.15), we get for the free-energy density:

$$\frac{\mathcal{F}}{n}=-\frac{1}{\kappa^2 t}\left[\tfrac{2}{3}T\sum_{\omega}(|\omega|+\Delta)^{3/2}+\tfrac{1}{2}u\left(T\sum_{\omega}\sqrt{|\omega|+\Delta}\right)^2\right]. \tag{4.17}$$

The equations (4.15), (4.16) and (4.17) are key results (Sachdev *et al.* 1995; Sengupta & Georges 1995), from which our mean-field predictions for physical observables

will follow. Despite their apparent simplicity, these results contain a great deal of structure, and a fairly careful and non-trivial analysis is required to extract the universal information contained within them.

First, it is easy to note that there is no sensible solution (with $\Delta > 0$) of (4.15) at $T = 0$ for $\tilde{r} < \tilde{r}_c$ where

$$\tilde{r}_c = u \int \frac{d\omega}{2\pi} \sqrt{|\omega|} \approx \frac{2\Lambda_\omega^{3/2}}{3\pi}, \tag{4.18}$$

where Λ_ω is an upper cut-off in frequency. Clearly the system is in the MSG phase for $T = 0$, $\tilde{r} < \tilde{r}_c$, and a separate ansatz for Q is necessary there, as discussed elsewhere (Sachdev *et al.* 1995). Let us now define

$$r \equiv \tilde{r} - \tilde{r}_c, \tag{4.19}$$

so that the quantum critical point is at $T = 0$, $r = 0$. In the vicinity of this point, our action constitutes a continuum quantum field theory (CQFT) describing the physics of the system at all energy scales significantly smaller than Λ_ω. The 'universal' properties of the system are the correlators of this CQFT, and they apply therefore for $r, T \ll \Lambda_\omega$, a condition we assume in our analysis below. It is also natural to assume that the microscopic coupling $u \sim \Lambda_\omega^{-1/2}$. We shall, however, make no assumptions on the relative magnitudes of r and T.

The general solution of (4.15) under the conditions noted above was described by Sachdev & Read (1996); we only present the final result for Δ, which is in the form of a solvable quadratic equation for $\sqrt{\Delta}$:

$$\Delta + uT\sqrt{\Delta} = r\left(1 - \frac{u\Lambda_\omega^{1/2}}{\pi}\right) + uT^{3/2}\,\Phi\left(\frac{r}{T}\right), \tag{4.20}$$

where the universal crossover function $\Phi(y)$ is given by

$$\Phi(y) = \frac{1}{\pi^2}\int_0^\infty \sqrt{s}\,ds\left[\log\left(\frac{s}{2\pi}\right) - \psi\left(1 + \frac{s+y}{2\pi}\right) + \frac{\pi + y}{s}\right], \tag{4.21}$$

with ψ the digamma function. The following limiting results, which follow from (4.21), are useful for our subsequent analysis:

$$\Phi(y) = \begin{cases} \sqrt{1/2\pi}\,\zeta(3/2) + \mathcal{O}(y), & y \to 0, \\ (2/3\pi)y^{3/2} + y^{1/2} + (\pi/6)y^{-1/2} + \mathcal{O}(y^{-3/2}), & y \to \infty. \end{cases} \tag{4.22}$$

The expression (4.16), combined with the results (4.20) and (4.21) completely specify the r and T dependence of the dynamic susceptibility in the MQP phase, and allow us to obtain the phase diagram shown in figure 5. The crossovers shown are properties of the CQFT characterizing the quantum critical point. We present below explicit results for the crossover functions of a number of observables within the mean-field theory.

Before describing the crossovers, we note that the full line in figure 5 denotes the boundary of the paramagnetic phase at $r = r_c(T)$ (or $T = T_c(r)$). This is the only line of thermodynamic phase transitions, and its location is determined by the condition $\Delta = 0$, which gives us

$$r_c(T) = -u\Phi(0)T^{3/2} \quad \text{or} \quad T_c(r) = (-r/u\Phi(0))^{2/3}. \tag{4.23}$$

The different regimes in figure 5 can be divided into two classes determined by

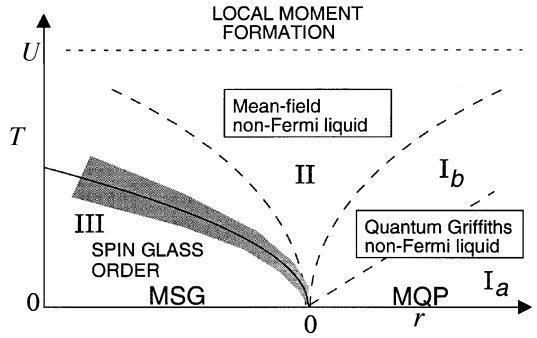

Figure 5. Phase diagram of a metallic spin glass as a function of the ground state tuning parameter, r, and temperature, T. The mean-field theory of local moment formation discussed in § 3 *b* applies at temperatures, T, greater than U for all values of r. In the notation of figure 1, the $T = 0$ state is a MSG for $r < 0$ and a MQP for $r > 0$. The full line is the only thermodynamic phase transition, and is at $r = r_c(T)$ or $T = T_c(r)$. The quantum critical point is at $r = 0$, $T = 0$, and is described by a continuum quantum field theory (CQFT). The dashed lines denote crossovers between different finite-T regions of the CQFT: the low-T regions are I*a*, I*b* (on the paramagnetic side) and III (on the ordered side), while the high-T region (II) displays 'mean-field non-Fermi liquid' behaviour. The quantum Griffiths precursors of the MSG phase occur in region I, and now rare regions lead to certain 'quantum Griffiths non-Fermi liquid' characteristics in the thermodynamics. The crossovers on either side of II, and the spin glass phase boundary $T_c(r)$, all scale as $T \sim |r|^{z\nu/(1+\theta_u\nu)}$; the boundary between I*a* and I*b* obeys $T \sim r^{z\nu}$. The mean-field values of these exponents are $z = 4$, $\nu = \frac{1}{4}$, and $\theta_u = 2$. The shaded region has classical critical fluctuations described by theories of the type discussed by Fischer & Hertz (1991).

whether T is 'low' or 'high'. There are two low-T regimes, one for $r > 0$, and the other for $r < 0$; these regions display properties of the non-critical ground states, which were reviewed in § 2. More novel is the high-T region, where the most important energy scale is set by T, and 'non-Fermi liquid' effects associated with the critical ground state occur. We now describes the regimes in more detail, in turn.

(i) *Low-T region above MQP ground state, $T < (r/u)^{2/3}$*

This is the mean-field 'Fermi-liquid' region, where the leading contribution to Δ is its $T = 0$ value $\Delta(T) \sim \Delta(0) = r$. The leading temperature dependent correction to Δ is however different in two subregions. In the lowest-T region Ia, $T < r$, we have the Fermi-liquid T^2 power law

$$\Delta(T) - \Delta(0) = \frac{u\pi T^2}{6\sqrt{r}} \quad \text{region I}a. \tag{4.24}$$

At higher temperatures, in region I*b*, $r < T < (r/u)^{2/3}$, we have an anomalous temperature dependence

$$\Delta(T) - \Delta(0) = u\Phi(0)T^{3/2} \quad \text{region I}b \text{ and II}. \tag{4.25}$$

It is also interesting to consider the properties of region I as a function of observation frequency, ω, as sketched in figure 6.

At large frequencies, $\omega \gg r$, the local dynamic susceptibility behaves like $\chi''_L \sim \mathrm{sgn}(\omega)\sqrt{|\omega|}$, which is the spectrum of critical fluctuations; at the $T = 0$, $r = 0$ critical point, this spectrum is present at all frequencies. At low frequencies, $\omega \ll r$, there is a crossover (figure 6) to the characteristic Fermi-liquid spectrum of local spin fluctuations $\chi''_L \sim \omega/\sqrt{r}$.

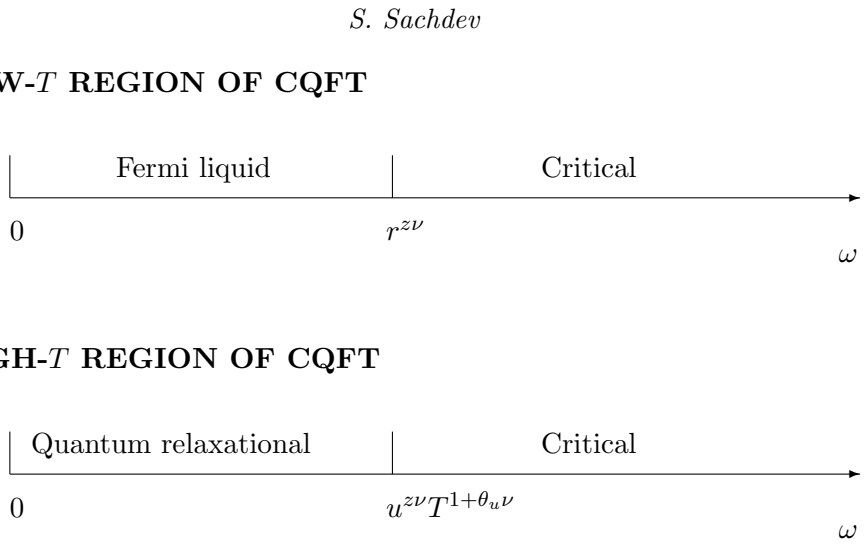

Figure 6. Crossovers as a function of frequency, ω, in the regions of figure 5. The low-T region is on the paramagnetic side ($r > 0$). The quantum Griffiths effects occur in the 'Fermi-liquid' region, making it the 'quantum Griffiths non-Fermi liquid' of figure 5.

The present mean-field theory of course does not contain Griffiths effects coming from rare local fluctuations. These were discussed in § 3 and, as noted there, are crucial in understanding the low-T properties of the MQP phase. The present mean-field theory captures the behaviour of a 'typical' region of the sample, but it is the rare regions that dominate the thermodynamics and lead to certain 'quantum Griffiths non-Fermi liquid' characteristics.

(ii) *High-T region, $T > (|r|/u)^{2/3}$*

This is the 'mean-field non-Fermi-liquid' region; unlike region (I), the non-Fermi liquid effects are now properties of the mean-field theory, and not consequences of rare fluctuations. Here temperature-dependent contributions to Δ dominate over those due to the deviation of the coupling r from its critical point, $r = 0$. Therefore thermal effects are dominant, and the system behaves as if its microscopic couplings are at those of the critical ground state. The T dependence in (4.25) continues to hold, as we have already noted, with the leading contribution now being $\Delta \approx u\Phi(0)T^{3/2}$. As in (I), it is useful to consider properties of this region as a function of ω (figure 6). For large ω ($\omega \gg uT^{3/2}$) we again have the critical behaviour $\chi_{\rm L}'' \sim \mathrm{sgn}(\omega)\sqrt{|\omega|}$; this critical behaviour is present at large enough ω in all the regions of the phase diagram. At small ω ($\omega \ll uT^{3/2}$), thermal fluctuations quench the critical fluctuations, and we have relaxational behaviour with $\chi_{\rm L}'' \sim \omega/u^{1/2}T^{3/4}$.

(iii) *Low-T region above MSG ground state, $T < (-r/u)^{2/3}$*

Effects due to the formation of a static moment are now paramount. As one approaches the spin glass boundary (4.23) from above, the system enters a region of purely classical thermal fluctuations, $|T - T_{\rm c}(r)| \ll u^{2/3}T_{\rm c}^{4/3}(r)$ (shown shaded in figure 5) where

$$\Delta = \left(\frac{r - r_{\rm c}(T)}{Tu}\right)^2. \tag{4.26}$$

Notice that Δ depends on the square of the distance from the finite-T classical phase-transition line, in contrast to its linear dependence, along $T = 0$, on the deviation from the quantum critical point at $r = 0$.

We have now completed a presentation of the mean-field predictions for the finite-T crossovers near the quantum critical point (figure 5), and for the explicit crossover functions for the frequency-dependent local dynamic susceptibility (figure 6 and equations (4.16), (4.20), (4.21)). We also summarize here results for a number of other experimental observables, whose T and r dependences follow from those of Δ described above.

Nuclear relaxation rate $1/T_1$ (Sengupta & Georges 1995):

$$\frac{1}{T_1 T} = A^2 \lim_{\omega \to 0} \frac{\chi''_{\mathrm{L}}(\omega)}{\omega} = \frac{A^2}{2\kappa\sqrt{\Delta}}, \tag{4.27}$$

where A is determined by the hyperfine coupling.

Uniform linear susceptibility, χ_u*:*

$$\chi_{\mathrm{u}} = \chi_{\mathrm{b}} - \frac{g}{t\kappa}\sqrt{\Delta}, \tag{4.28}$$

where χ_{b} is the T- and r-independent background contribution of the fermions that have been integrated out, g is a coupling constant.

Nonlinear susceptibility χ_{nl}*:*

$$\chi_{\mathrm{nl}} = \frac{ug^2}{4t}\frac{1}{\Delta}. \tag{4.29}$$

Notice that χ_{nl} is proportional to the quantum-mechanical interaction u and would vanish in a theory with terms associated only with disorder fluctuations.

Free energy and specific heat: the result for the free energy was given in (4.17), and it needs to be evaluated along the lines of the analysis carried out above for the crossover function determining Δ. Such a calculation gives

$$\frac{\mathcal{F}(T,r) - \mathcal{F}(T=0,r=0)}{n} = -\frac{1}{\kappa^2 t}\left[\frac{2r\Lambda_\omega^{3/2}}{3\pi} + T^{5/2}\Phi_{\mathcal{F}}\left(\frac{\Delta}{T}\right) + \frac{\Lambda_\omega\Delta^2}{2\pi} + \frac{(\Delta - r)^2}{2u} - \frac{4\Delta^{5/2}}{15\pi}\right], \tag{4.30}$$

where

$$\Phi_{\mathcal{F}}(y) = -\frac{2\sqrt{2}}{3\pi}\int_0^\infty \frac{\mathrm{d}\Omega}{\mathrm{e}^\Omega - 1}\frac{\Omega(2y + \sqrt{\Omega^2 + y^2})}{\sqrt{y + \sqrt{\Omega^2 + y^2}}}. \tag{4.31}$$

This result for $\mathcal{F}$ includes non-singular contributions, smooth in r, which form a background to the singular critical contributions. In region II, the most singular term is the one proportional to $\Phi_{\mathcal{F}}$, and yields a specific heat, C_{v} (Sengupta & Georges 1995):

$$\frac{C_{\mathrm{v}}}{T} = \gamma_{\mathrm{b}} - \frac{\zeta(\frac{5}{2})}{\sqrt{2\pi}\kappa^2 t}\sqrt{T}, \tag{4.32}$$

where γ_{b} is a background contribution.

Charge transport: the consequences of the order parameter fluctuations on charge transport were explored by Sengupta & Georges (1995). The quasi-particles are assumed to carry both charge and spin and they scatter off the spin fluctuations

via an exchange coupling. In the Born approximation, this leads to a contribution to the quasi-particle relaxation rate, $1/\tau_{\rm qp}$

$$\frac{1}{\tau_{\rm qp}} \propto \int_0^\infty \frac{{\rm d}\Omega}{\sinh(\Omega/T)} \frac{\Omega}{\sqrt{\Delta + \sqrt{\Omega^2 + \Delta^2}}}, \tag{4.33}$$

whose T and r dependence follows from that of Δ. In region II, $1/\tau_{\rm qp} \sim T^{3/2}$.

(*d*) *Application to experiments*

There has been much recent experimental activity on the transport, thermodynamic and neutron scattering properties of a number of rare-earth intermetallic compounds which diplay low T 'non-Fermi-liquid' behaviour. A majority of these systems are not too far from a magnetically ordered phase of some type: spin glass ordering has been observed in $Y_{1-x}U_xPd_3$ (Gajewski *et al.* 1996), $La_{1-x}Ce_xCu_{2.2}Si_2$ (Steglich *et al.* 1996), and URh_2Ge_2 (Sullow *et al.* 1997). However, it is fair to say that a direct relationship between the properties of these materials and the complicated theoretically predicted set of crossovers in figure 5 has not yet been clearly established. The material $La_{1-x}Ce_xCu_{2.2}Si_2$ has been studied in region II of figure 5 (Steglich *et al.* 1996) and it appears that initial results for the resistivity and the specific heat agree well with the mean-field theoretical predictions reviewed in § 4 *c*.

5. Conclusions

In a recent conference on 'non-Fermi-liquid behaviour in metals' (Coleman *et al.* 1996), two routes to non-Fermi-liquid behaviour were discussed: those due to so-called Kondo disorder models and those due to proximity to a magnetic quantum phase transition. These were viewed as competing mechanisms which possibly applied to different rare-earth intermetallic compounds. One of the purposes of this article has been to argue that these mechanisms are really better viewed as different limiting regimes of the same underlying physics and that no material is strictly in one or the other regime. Our basic point is made clear by a glance at figure 5. The Kondo disorder models apply at low T above the MQP ground state: here rare local moments with anomalously low Kondo temperatures appear to dominate and lead to non-Fermi-liquid effects. We have argued here that these effects are best viewed as quantum Griffiths singularities associated with the transition to the MSG phase (or in more regular systems, as a transition to some ordered metallic antiferromagnet), and they are denoted in figure 5 as 'quantum Griffiths non-Fermi liquid'. The other region of non-Fermi-liquid behaviour appears in region II, describable as the high-T region of the CQFT associated with the MQP–MSG quantum critical point. Now the non-Fermi-liquid behaviour is associated with the behaviour of the typical local moment and is accessible in mean-field theory; this is denoted in figure 5 as 'mean-field non-Fermi liquid'. Clearly the fluctuation terms which disrupted the mean-field predictions in region I are also going to be significant here, but there is no clear understanding of their structure. A unified theoretical description which includes such corrections and the crossover to the quantum Griffiths singularities in region I is lacking, and should be an important focus of future theoretical work.

I thank T. Senthil for a recent collaboration (Senthil & Sachdev 1997) and for helpful remarks which greatly influenced the perspective of this article. The research was supported by the US National Science Foundation under grant number DMR-96-23181.

References

Alloul, H. & Dellouve, P. 1987 Spin localization in Si:P—direct evidence from ^{31}P nuclear magnetic resonance. *Phys. Rev. Lett.* **59**, 578–581.

Altshuler, B. L. & Aronov A. G. 1983 Fermi-liquid theory of the electron–electron interaction effects in disordered metals. *Sol. State. Comm.* **46**, 429–435.

Anderson, P. W. 1961 Localized magnetic states in metals. *Phys. Rev.* **124**, 41–53.

Belitz, D. & Kirkpatrick, T. R. 1994 The Anderson–Mott transition. *Rev. Mod. Phys.* **66**, 261–380.

Bhatt, R. N. & Fisher, D. S. 1992 Absence of spin diffusion in most random lattices. *Phys. Rev. Lett.* **68**, 3072–3075.

Bhatt, R. N. & Lee, P. A. 1982 Scaling studies of highly disordered spin-$\frac{1}{2}$ antiferromagnetic systems. *Phys. Rev. Lett.* **48**, 344–347.

Binder, K. & Young, A. P. 1986 Spin glasses: experimental facts, theoretical concepts, and open questions. *Rev. Mod. Phys.* **58**, 801–976.

Bray, A. J. & Moore, M. A. 1980 Replica theory of quantum spin glasses. *J. Phys.* C **13**, L655–660.

Castellani, C. & DiCastro, C. 1985 Metal–insulator transition and Landau Fermi liquid theory. In *Localization and the metal–insulator transition* (ed. H. Fritzsche & D. Adler). New York: Plenum.

Coleman, P., Maple, B. & Millis, A. 1996 Institute for theoretical physics conference on non-Fermi liquid behavior in metals. *J. Phys. Condens. Matter* **8**(48).

Dasgupta, C. & Ma, S.-K. 1980 Low temperature properties of the random Heisenberg antiferromagnetic chain. *Phys. Rev.* B **22**, 1305–1319.

Dobrosavljevic, V., Kirkpatrick, T. R. & Kotliar, G. 1992 Kondo effect in disordered systems. *Phys. Rev. Lett.* **69**, 1113–1116.

Dobrosavljevic, V. & Kotliar, G. 1993 Hubbard models with random hopping in $d = \infty$. *Phys. Rev. Lett.* **71**, 3218–3221.

Finkelstein, A. M. 1983 Influence of Coulomb interaction on the properties of disordered metals. *Zh. Eksp. Teor. Fiz.* **84**, 168–189. (*Sov. Phys.-JETP* **57**, 97–108.)

Finkelstein, A. M. 1984 Weak localization and Coulomb interaction in disordered systems. *Z. Phys.* B **56**, 189–196.

Fischer, K. H. & Hertz, J. A. 1991 *Spin glasses*. Cambridge University Press.

Fisher, D. S. 1992 Random transverse field Ising spin chain. *Phys. Rev. Lett.* **69**, 534–537.

Fisher, D. S. 1995 Critical behavior of random transverse-field Ising spin chains. *Phys. Rev.* B **51**, 6411–6461.

Fisher, M. E. 1978 Yang–Lee edge singularity and φ^3 field theory. *Phys. Rev. Lett.* **40**, 1610–1613.

Gajewski, D. A., Dilley, N. R., Chau, R. & Maple, M. B. 1996 Non-Fermi liquid and magnetic behavior of the $Y_{1-x}U_xPd_3$ system. *J. Phys. Condens. Matter* **8**, 9793–9806.

Guo, M., Bhatt, R. N. & Huse, D. A. 1996 Quantum Griffiths singularities in the transverse field Ising spin glass. *Phys. Rev.* B **54**, 3336–3342.

Haldane, F. D. M. 1978 Scaling theory of the asymmetric Anderson model. *Phys. Rev. Lett.* **40**, 416–419.

Hertz, J. A. 1979 The Stoner glass. *Phys. Rev.* B **19**, 4796–4804.

Hirsch, J. E. 1980 Low-temperature thermodynamic properties of a random anisotropic antiferromagnetic chain. *Phys. Rev.* B **22**, 5355–5365.

Krishnamurthy, H. R., Wilkins, J. W. & Wilson, K. G. 1980 Renormalization-group approach to the Anderson model of dilute magnetic alloys. *Phys. Rev.* B **21**, 1003–1083.

Lakner, M., Lohneysen, H. v., Langenfeld, A. & Wolfle, P. 1994 Localized magnetic moments in Si:P near the metal–insulator transition. *Phys. Rev.* B **50**, 17 064–17 073.

Lamelas, F. J., Werner, S. A., Shapiro, S. M. & Mydosh, J. A. 1995 Intrinsic spin-density-wave magnetism in Cu–Mn alloys. *Phys. Rev.* B **51**, 621–624.

Langenfeld, A. & Wolfle, P. 1995 Disorder-induced local magnetic moments in weakly correlated metallic systems. *A. Phys.* **4**, 43–52.

Ma, S.-K., Dasgupta, C. & Hu, C.-K. 1979 Random antiferromagnetic chain. *Phys. Rev. Lett.* **43**, 1434–1437.

Milovanovic, M., Sachdev, S. & Bhatt, R. N. 1989 Effective field theory of local moment formation in disordered metals. *Phys. Rev. Lett.* **63**, 82–85.

Huse, D. A. & Miller, J. 1993 Zero-temperature critical behavior of the infinite-range quantum Ising spin glass. *Phys. Rev. Lett.* **70**, 3147–50.

Miranda, E., Dobrosavljevic, V. & Kotliar, G. 1996 Kondo disorder: a possible route towards non-Fermi-liquid behavior. *J. Phys. Condens. Matter* **8**, 9871–9900.

Miranda, E., Dobrosavljevic, V. & Kotliar, G. 1997 Disorder-driven non-Fermi liquid behavior in Kondo alloys. *Phys. Rev. Lett.* **78**, 290–293.

Oppermann, R. & Binderberger, M. 1994 Solution for the $T = 0$ quantum spin glass transition in a metallic model with spin-charge coupling. *Ann. Physik.* **3**, 494

Quirt, J. D. & Marko, J. R. 1971 Electron-spin-resonance measurements of the spin susceptibility of heavily doped n-type silicon. *Phys. Rev. Lett.* **26**, 318–321.

Read, N., Sachdev, S. & Ye, J. 1995 Landau theory of quantum spin glasses of rotors and Ising spins. *Phys. Rev.* B **52**, 384–410.

Rowan, D. G., Szczech, Y. H., Tusch, M. A. & Logan, D. E. 1995 Magnetic response of local moments in disordered metals. *J. Phys. Condens. Matter* **7**, 6853–6868.

Sachdev, S. 1989 Local moments near the metal–insulator transition. *Phys. Rev.* B **39**, 5297–5310.

Sachdev, S. 1995 Quantum phase transitions in spin systems and the high temperature limit of continuum quantum field theories. In *Proc. 19th IUPAP Int. Conf. on Statistical Physics, Xiamen, China.* Singapore: World Scientific.

Sachdev, S. & Read, N. 1996 Metallic spin glasses. *J. Phys. Condens. Matter* **8**, 9723–9741.

Sachdev, S & Ye, J. 1992 Universal quantum-critical dynamics of two dimensional antiferromagnets. *Phys. Rev. Lett.* **69**, 2411–2414.

Sachdev, S. & Ye, J. 1993 Gapless spin-fluid ground state in a random quantum Heisenberg magnet. *Phys. Rev. Lett.* **70**, 3339–3342.

Sachdev, S., Read, N. & Oppermann, R. 1995 Quantum field theory of metallic spin glasses. *Phys. Rev.* B **52**, 10 286–10 294.

Sengupta, A. & Georges, A. 1995 Non-Fermi-liquid behavior near a $T = 0$ spin glass transition. *Phys. Rev.* B **52**, 10 295–10 302.

Senthil, T. & Sachdev, S. 1996 Higher dimensional realization of activated dynamic scaling at random quantum transitions. *Phys. Rev. Lett.* **77**, 5292–5295.

Steglich, F., Buschinger, B., Gegenwart, P., Lohmann, M., Helfrich, R., Langhammer, C., Hellmann, P., Donnevert, L., Thomas, S., Link, A., Geibel, C., Lang, M., Sparn, G. & Assmus, W. 1996 Quantum critical phenomena in undoped heavy-fermion metals. *J. Phys. Condens. Matter* **8**, 9909–9922.

Sullow, S., Nieuwenhuys, G. J., Menovsky, A. A., Mydosh, J. A., Mentink, S. A. M., Mason, T. E. & Buyers, W. J. L. 1997 Spin glass behavior in URh_2Ge_2. *Phys. Rev. Lett.* **78**, 354–357.

Thill, M. J. & Huse, D. A. 1995 Equilibrium behavior of quantum Ising spin glass. *Physica* **214A**, 321–355.

Tusch, M. A. & Logan, D. E. 1993 Interplay between disorder and electron interactions in a $d = 3$ site-disordered Anderson–Hubbard model: a numerical mean-field study. *Phys. Rev.* B **48**, 14 843–14 858.

Tusch, M. A. & Logan, D. E. 1995 Disorder-induced fluctuations in the magnetic properties of an Anderson–Hubbard model. *Phys. Rev.* B **51**, 11 940–11 943.

Ue, S. & Maekawa, S. 1971 Electron-spin-resonance studies of heavily phosphorus-doped silicon *Phys. Rev.* B **3**, 4232–4238.

Wolff, P. A. 1961 Localized moments in metals. *Phys. Rev.* **124**, 1030–1035.

Ye, J., Sachdev, S. & Read, N. 1993 Solvable spin glass of quantum rotors. *Phys. Rev. Lett.* **70**, 4011–4014.

Discussion

H. VON LÖHNEYSEN (*Institute of Physics, University of Karlsruhe, Germany*). The temperature dependence of the resistivity (about $T^{3/2}$) and specific heat coefficient (about $T^{1/2}$) at the quantum critical point of your spin glass model are the same as those of spin fluctuation models, for instance by Millis. Is this a coincidence or is there a deeper relation between both models? How about the temperature dependence of the other quantities T_1 and χ that was mentioned?

S. SACHDEV. The density of states of spin fluctuations is the same in our mean-field theory for the spin glass transition and the ordered metallic magnet transitions in three dimensions. I believe this is a coincidence. Our mean-field results are dimension independent, while those of Millis are not. Physical quantities which can be directly related to this density of states will therefore be the same in the two cases, but others do have a different temperature dependence. So T_1 is the same, but I believe χ is different.

PHILOSOPHICAL TRANSACTIONS OF THE ROYAL SOCIETY A MATHEMATICAL, PHYSICAL & ENGINEERING SCIENCES

PHILOSOPHICAL TRANSACTIONS OF THE ROYAL SOCIETY A MATHEMATICAL, PHYSICAL & ENGINEERING SCIENCES